*Annals of Biomedical Engineering*, Vol. 45, No. 9, September 2017 (© 2017) pp. 2088–2097
DOI: 10.1007/s10439-017-1845-1

# Real-Time Prediction of Temperature Elevation During Robotic Bone Drilling Using the Torque Signal

ARNE FELDMANN,[1] KATE GAVAGHAN,[2,3] MANUEL STEBINGER,[2,3] TOM WILLIAMSON,[2,3] STEFAN WEBER,[2,3] and PHILIPPE ZYSSET[1]

[1]Institute for Surgical Technology and Biomechanics, Stauffacherstr. 78, 3014 Bern, Switzerland; [2]ARTORG Center for Biomedical Engineering Research, Murtenstr. 50, 3010 Bern, Switzerland; and [3]University of Bern, Bern, Switzerland

(*Received 25 November 2016; accepted 26 April 2017; published online 5 May 2017*)

Associate Editor Mona Kamal Marei oversaw the review of this article.

**Abstract**—Bone drilling is a surgical procedure commonly required in many surgical fields, particularly orthopedics, dentistry and head and neck surgeries. While the long-term effects of thermal bone necrosis are unknown, the thermal damage to nerves in spinal or otolaryngological surgeries might lead to partial paralysis. Previous models to predict the temperature elevation have been suggested, but were not validated or have the disadvantages of computation time and complexity which does not allow real time predictions. Within this study, an analytical temperature prediction model is proposed which uses the torque signal of the drilling process to model the heat production of the drill bit. A simple Green's disk source function is used to solve the three dimensional heat equation along the drilling axis. Additionally, an extensive experimental study was carried out to validate the model. A custom CNC-setup with a load cell and a thermal camera was used to measure the axial drilling torque and force as well as temperature elevations. Bones with different sets of bone volume fraction were drilled with two drill bits (∅1.8 mm and ∅2.5 mm) and repeated eight times. The model was calibrated with 5 of 40 measurements and successfully validated with the rest of the data ($R^2 = 0.9034$, $SEE = 7.582\,^{\circ}\mathrm{C}$). It was also found that the temperature elevation can be predicted using only the torque signal of the drilling process. In the future, the model could be used to monitor and control the drilling process of surgeries close to vulnerable structures.

**Keywords**—Bone drilling, Temperature prediction model, Drilling model, Force–torque model, Temperature elevation during bone drilling, Bone necrosis, Thermal tissue damage.

## INTRODUCTION

Bone drilling is a frequently utilized surgical task in a number of medical domains including orthopedic surgery, dentistry, neurosurgery and head and neck surgery. Due to the risk posed to surrounding tissue due to thermal damage, a recent scientific effort to optimize and model the drilling process has been undertaken. Unlike metal, human bone has a low thermal conductivity[5] which confines and accumulates drilling heat within a small region around the drilled hole. It is not known if bone damage causes long term complications in orthopedic surgeries (e.g., screw loosening), it was found that it affects the osseointegration of dental implants.[26] It is even more problematic if the bone drilling occurs in close proximity to more vulnerable structures such as nerves. This is because the thermal damage of a bone cutting process can lead to permanent nerve damage.[13]

A newly described approach to the inner ear for cochlear implantation, in which a direct tunnel is drilled using stereotactic guidance through the close lying nerves of the facial recess (facial nerve and chorda tympani), is a procedure in which a drill bit may possibly be required to pass within 0.5 mm from nerve tissue.[2] Recent studies have shown, that drilling this access might lead to thermal damage of the facial nerve and thus partial or complete unilateral paralysis or paresis of the facial muscles.[7,13] However, efforts have been made to reduce this risk by optimizing drill bit design and drilling process parameters.[8]

In general, there has been a great effort in investigating bone drilling as reviewed and summarized by multiple authors.[1,3,21] The previous work suggests a low rotational speed (ca. 1000 RPM) and a high feed rate (ca. 1 mm/s) with sufficient irrigation helps to

Address correspondence to Arne Feldmann, Institute for Surgical Technology and Biomechanics, Stauffacherstr. 78, 3014 Bern, Switzerland. Electronic mail: arne.feldmann@istb.unibe.ch

minimize the temperature elevation. While optimizing the drilling process for heat is important, a thermal model that would enable the real time prediction of thermal elevation during a surgical procedure which is additionally dependent on case specific factors such as bone density, could aid in reducing the occurrence of thermal damage.

There have been several attempts at modeling the drilling process with focus on either the prediction of cutting forces[14,16,24] or temperatures. Temperature prediction approaches can be divided into more analytical[15,17] or more numerical (FEM) approaches[23,25,27] as reviewed by Marco *et al.*[18] In the analytical thermal models combined heat-equations for the interaction of drill bit, bone chips, cooling (irrigation) and surrounding bone are solved, but were not validated and require many prior assumptions. Some previously described FEM models have been validated, but temperature elevation for only a few millimeters drilling depth can be calculated and like other mentioned models, are very time consuming to compute.

To enable temperature elevation prediction based on real time measured parameters, this work focuses on the development of a new model that allows for real time calculations during the drilling process. In our previous research,[7] an analytical model with only two calibration constants was developed to allow prediction of the temperature elevation based on the bone density distribution along the drilling trajectory. It was assumed that density of the bone relates in a power function to the drilling force. A moving point source Green's function was then used to calculate the temperature elevation at a point in space over time.

This model has been used with overall good results in an *in vivo* sheep study for the access drilling of minimally invasive robotic cochlear implantation. However, while bone density can be determined pre-operatively from medical images, in a real surgical procedure, the absolute prediction of the drilling path and thus, the bone density profile through which the drilling is being conducted, is not possible. Additionally, case specific factors such as drill bit wear or tissue becoming jammed in the drill bit flukes can also significantly and rapidly effect the thermal elevation.

In this study we introduce and validate an improved version of this model which uses the torque, easily sensed data during surgical drilling, to calculate the temperature elevation for drill bits with different diameters in real time. In the future, this model might help to monitor and control the temperature elevation of the drilling process for more delicate surgeries like the minimally invasive robotic cochlear implantation.

## MATERIALS AND METHODS

The previously introduced model [7] to predict temperature elevation based on bone density information along the drilling trajectory was modified to allow the real-time prediction of temperature elevation during the drilling process. After the derivation of this model, a custom designed experimental setup is described which is then used to conduct a large set of experiments in order to evaluate the proposed model.

### *Temperature Prediction Model*

The previous approach required preoperative image information about bone densities which were assumed to relate to the axial drilling forces at each drilling depth [$F(t) \sim Density(t)^b$; with $b \approx 1.8$]. This approach relied therefore on the quality of CT images and knowledge of the drilling path pre-operatively (i.e., does not account for drill positioning errors). The new model does not require prior knowledge of the drilling path but instead takes advantage of drilling forces and torques. The model thus additionally incorporates information pertaining to the density of bone through which the drill is passing (e.g., for tool tracking[29]) and other influences on temperature prediction such as flute clogging.

Therefore, the bone density information was not considered but the axial torque [$M(t)$ in (Nm)] is used to directly calculate the energy (heat) function [$\dot{Q}(t)$ in (W)]. Only the torque and not the thrust force was used because its contribution is very small and the torque in general relates better to the cutting work of drilling.[12] In this simplified method, it is assumed that all the energy is produced at the tip of the drill bit and not at the side. Additionally, the three dimensional shape of the tip and cutting edges are averaged into a two dimensional disk. It was a posteriori found that this simplification does not significantly influence the accuracy of the temperature prediction.

The energy (heat) source was then first derived from the work of the cutting process:

$$\dot{Q}(t) = M(t) \cdot \omega \cdot \left(\frac{M(t)}{M_0}\right)^{(b-1)}. \qquad (1)$$

With $M_0$ in (Nm) and $b$ being dimensionless are calibration constants which describe the fraction of mechanical energy which is converted to heat and transferred into the system (bone). The rotational speed $\left(\omega = 2\pi\frac{n}{60}\ with\ n = 1000\ RPM\right)$ is constant. The energy contribution from the thrust force is not considered because it is much smaller than the torque contribution. As described in Ref. 7, the temperature elevation in a material at a given point $(x, y, z)$ can

then be evaluated using a continuous but varying moving point source Green's function:

$$T(t,x,y,z) = T_0 + \int_0^t \frac{\dot{Q}_{Point}(\tau)}{8\rho c_p(\pi\alpha\tau)^{\frac{3}{2}}} \cdot e^{-\frac{(x-x_0)^2+(y-y_0)^2+(z-z_0-v\tau)^2}{4\alpha\tau}} d\tau. \tag{2}$$

The coordinates $x_0$, $y_0$, $z_0$ describe the initial position of the point source which resembles the starting point of the drilling. To account for different drill bit diameters ($\emptyset$), Eq. (1) is normalized with the area of each drill bit and therefore expressed as heat flux (W/m$^2$):

$$J(t) = \frac{\dot{Q}(t)}{\pi\left(\frac{\emptyset}{2}\right)^2}. \tag{3}$$

This formula was modified from a point source to a disk source with the size of the drill bit diameter as seen in Fig. 1. For this, the heat flux (3) should be symmetrically distributed into a ring source with differential thickness $dr$ around the drilling axis which will be later integrated up to the total radius $R$ of each drill bit:

$$\dot{Q}_{Disk}(t) = \int_0^R \int_0^{2\pi} J(t)\,dA, \tag{4}$$

with $dA = \tilde{r} \cdot d\varphi \cdot d\tilde{r}$ The integration over the drill bit radius $r\,(from\,0\,to\,R = \frac{\emptyset}{2})$ and around the drilling axis $\varphi$ (from 0 to $2\pi$) can be expressed in polar coordinates. The distance $D$ between the point of temperature evaluation and the source location was also transformed to polar coordinates:

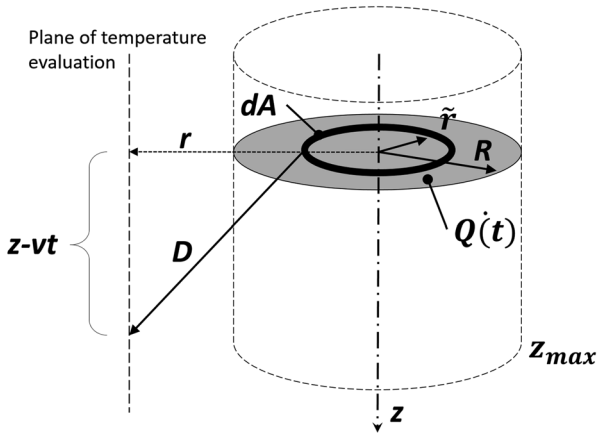


**FIGURE 1. Schematic view of disk source model and plane of temperature evaluation. The disk source is essentially an integration of a ring source up to the radius "R" of each drill bit.**

$$D^2 = (x-x_0)^2+(y-y_0)^2+(z-z_0)^2 = r^2 + \tilde{r}^2 - 2r\tilde{r}\cos(\varphi-\tilde{\varphi}) + (z-vt)^2.$$

Due to the axial symmetry, Eq. (2) was further modified and simplified to:

$$T(r,\,z,\,t) = T_0 + \int_0^{\frac{\emptyset}{2}} \int_0^t \frac{J(\tau)\tilde{r}}{4\sqrt{\pi}\rho c_p(\alpha\tau)^{\frac{3}{2}}} \cdot e^{-\frac{r^2+\tilde{r}^2+(z-z_0-v\tau)^2}{4\alpha\tau}} \cdot I_0\left(\frac{r\tilde{r}}{2\alpha\tau}\right) d\tau d\tilde{r}, \tag{5}$$

as suggested by Paek *et al.*[19,20] for the laser drilling process. With $I_0$ as the Bessel function of first kind and zeroth order and $T_0$ set to 25 °C room temperature. The $r$ polar coordinate is the distance to the drilling axis at which the temperatures are evaluated is set to match the plane of the thermal camera measurements $\left(\frac{\emptyset}{2} + 0.5\,mm\right)$.

Temperature elevations are evaluated at multiple depths from 0 to maximal drilling depth ($z_{max}$) in steps of $p_z = \frac{z_{max}}{n}$ ($z_{max} = 10$ or 20 mm, respectively and $n = 20$). The denominator "n" can be choosen to modify the spatial resolution of the temperature prediction. The constant thermal diffusivity $\alpha = \frac{k}{\rho c_p}$ in $m^2/s$ is calculated with material constants of compact cortical bone: $k = 0.55$ W/m/K;[5] $\rho = 1800$ kg/$m^3$; $c_p = 1260$ J/kg/K.[4] Due to the low homogeneous thermal conductivity of bone and therefore confined space of temperature elevation, constant room temperature and infinite boundaries were assumed.

### *Experimental Setup*

A custom experimental setup was used to measure axial drilling forces, torques and temperature elevations. Figure 2 shows the setup which consists of a programmable CNC-machine (3-axis Miniflat i-TM 100-2, ISEL, Germany), a motor spindle (BFS-8015-12, Mechatron GmbH, Germany), a thermal (infrared) camera (A655sc, FLIR, USA) with a macroscopic lens (for 50 $\mu$m resolution) and a load cell (F310-400N-2Nm, Novatech, UK). For the irrigation, a surgical roller pump (IRRIG PP980, Bien Air, Switzerland; not shown in Fig. 2) with standard irrigation tube (Bien Air, Switzerland) was used, allowing for the application of different flow rates.

The emissivity constant of the bone's surface was previously experimentally determined as $\varepsilon = 0.96$.[9] For the irrigation, a standard 19 gauge needle (inner diameter $\emptyset$0.686 mm) was bent such that the water jet hits the tip of the drill bit with an angle that is

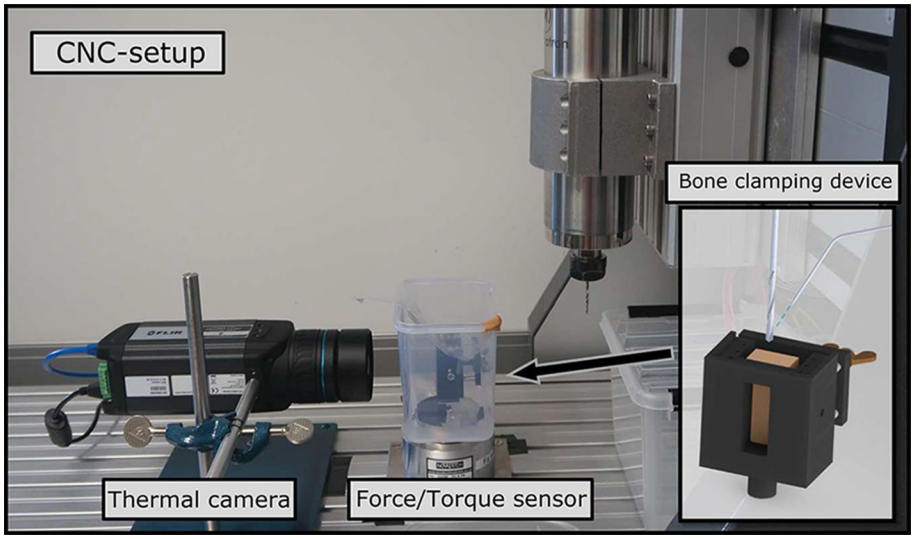


**FIGURE 2. Experimental 3-axis CNC-setup for measuring the temperature elevation, thrust force and torque during the drilling process. A macroscopic lens (50 $\mu$m) was used with the thermal camera. External irrigation and bone clamping device are shown in detail.**

approximately equivalent to the helix angle of the drill bit to allow cleaning of the flutes from bone chips. The irrigation fluid (water at 25 °C room temperature) is collected in the collection tank and can flow into a second container (not visible in Fig. 2).

### *Sample Preparation*

For these experiments, fresh bovine tibiae of 4-year-old (dairy) cows were acquired from a local slaughterhouse because they are largely available and optimal in size. The samples were frozen (−20 °C) and pre-cut using a hand saw. Saline solution was used for irrigating the sample preparation process. A diamond band saw (Exakt Advanced Technologies GmbH, Germany) was used to create one smooth surface to allow thermal imaging measurements.

The samples were prepared to mimic the pneumatised bone of the human mastoid (in which the facial recess, through which drilling in a robotic cochlear implantation occurs, lies). The temporal bone consists of bone with a different number of air cells and therefore varying levels of pneumatisation.[10] To represent air cells, lateral holes (∅1.5 mm) were drilled with perpendicular crossing axes to the intended drilling trajectory as shown in Fig. 3. Cancellous bone samples with different volume fractions were not used because of the marrow in-between trabeculae. This would be however an interesting experiment for future research.

To represent the varying levels of pneumatisation that occurs amongst the population, three sets of $N = 16$ samples were created with through-hole spacing of $d = 0.5$, 1.5 and 2.5 mm, respectively. The preparation enabled drilling to be performed along various controlled bone density profiles while maintaining the integrity of the samples' measurement surface (as may not be the case if real mastoid samples were utilized). The first 3 mm of the drilling sample was intentionally left as cortical layer to further mimic the mastoid bone. Above this 3 mm cortical bone layer, 5 mm of cortical bone was pre-drilled with a larger drill bit allow the thermal monitoring of the drilling to commence at the height of view of the thermal camera. The top remaining surrounding bone was used to seal the sample to its holder to prevent water flow over the field of view of the thermal camera. Each sample was positioned in the experimental setup such that the edge of the drilled hole was 0.5 mm from the plane of the thermal imaging. The samples were refrozen and thawed for at least 4 h in saline solution prior to the experiments. The average room temperature was measured to be 25 °C.

### *Experimental Procedure*

Custom made single cutting edge drill bits with a rake angle of 35° (canon drills with a helix, Louis Belet, Switzerland) with two different diameters (∅1.8 mm and ∅2.5 mm) were used. This drill bit has been designed to reduce temperature elevation while improving drilling accuracy. This design facilitates the cutting with one cutting edge and therefore minimizes the chisel edge.

The above mentioned three different sets of bones were drilled with a constant rotational speed ($n = 1000$

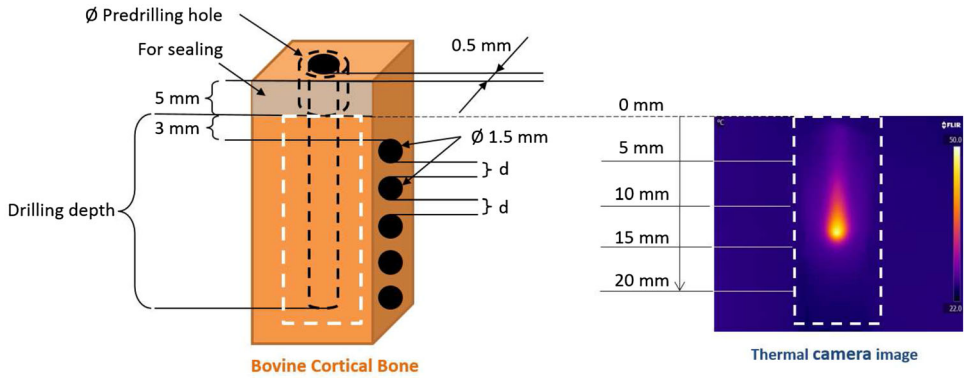


**FIGURE 3. Detailed view of bone sample dimensions, drilling depth and thermal camera image (50 μm). The distance between the edge of the drilling trajectory and the surface of thermal imaging is for both diameters 0.5 mm. The distance between the lateral through holes (∅1.5 mm) is denoted with "d" and varied for different sets of bone volume fraction (see experimental plan). The first 5 mm were pre-drilled with a larger diameter drill bit to allow fixation of the bone sample to prevent water leakage onto the field of view of the thermal camera. The actual first 3 mm of the drilling trajectory are intended to mimic the outer part of the human skull.**

**TABLE 1. Experimental plans for the three different sets of bone anatomy depicted in Fig. 3.**

| | Set 1 $d = 0.5$ mm | Set 2 $d = 1.5$ mm | Set 3 $d = 2.5$ mm |
|---|---|---|---|
| ∅1.8 mm | 10 mm | 10 mm | 10 mm |
| ∅2.5 mm | 20 mm | 20 mm | NA |

Values indicate the drilling depth for each combination of bone and drill bit diameter. Each parameter combination was repeated eight times (=40 experiments). Set 3 was not drilled with the 2.5 mm drill bit because of the excessive temperature rise due to drill bit flute jamming..

RPM) and a constant feed rate ($v = 0.5$ mm/s) with both drill bits. The constant irrigation rate was set to 15 mL/min and lateral holes were sealed with bone wax (Ethicon, USA) to prevent water penetration. Drillings were repeated eight times for each parameter combination (see Table 1). Set 3 was not drilled with the 2.5 mm drill bit due to excessive temperature rise due to drill bit flute jamming.

During drilling, the temperature of the prepared bone surface was recorded with the thermal camera (50 μm resolution; 12.5 fps) along with the applied force and torque (with 200 ms frequency). To compare thermal model and thermographic measurements, the maximum temperature over time was extracted from the thermal camera videos (ResearchIR, Flir, USA).

## RESULTS

The maximum temperature rise occurs at the tip region and is therefore a function of the advancing drill bit. The constants were calibrated ($M_0 = 100$ Nm and $b = 1.2$) by minimizing the mean distance of modeled and measured temperature elevations using one randomly selected measurement from each set (5 of 40 measurements). Figure 4 shows an example of the calculated temperatures in $p_z = 1$ mm steps over time and drilling depth of the drilling process using the ∅2.5 mm drill bit.

As mentioned, the maxima of the temperature curves at each depth coincide with the tip of the drill bit moving into the material. In order to compare temperature predictions to measurements, maximum temperature elevations over time are extracted both from model and thermal camera videos as seen in Fig. 5. Figure 5 shows one example for each drill bit diameter for sets 1 and 2. The bottom left picture is the extracted maximum from the same drilling as shown in Fig. 4.

To evaluate the model, temperatures in $p_z$ steps for both the model predicted and measured temperatures up to the maximal drilling depth were extracted. For all samples except those used for the calibration, the regression line, 95% prediction and confidence intervals, as well as adjusted R-square ($R^2 = 0.9034$) and the standard error of the estimates ($SEE = 7.682\,^{\circ}$C) were calculated and are shown in Fig. 6 (RStudio 3.2.5, USA). Model predictions showed a greater accuracy at lower temperatures (up to ca. 55 °C from room temperature $\Delta T = 30\,^{\circ}$C).

Additionally, the model was used to calculate examples of the temperature drop over the distance to the edge of the drilled hole $\left(r - \frac{\emptyset}{2}\right)$ as shown in Fig. 7. This graph highlights that there is a large temperature drop within only a few millimeters to the drilled hole which is due to the low thermal conductivity of bone. Measured and evaluated temperatures should there-

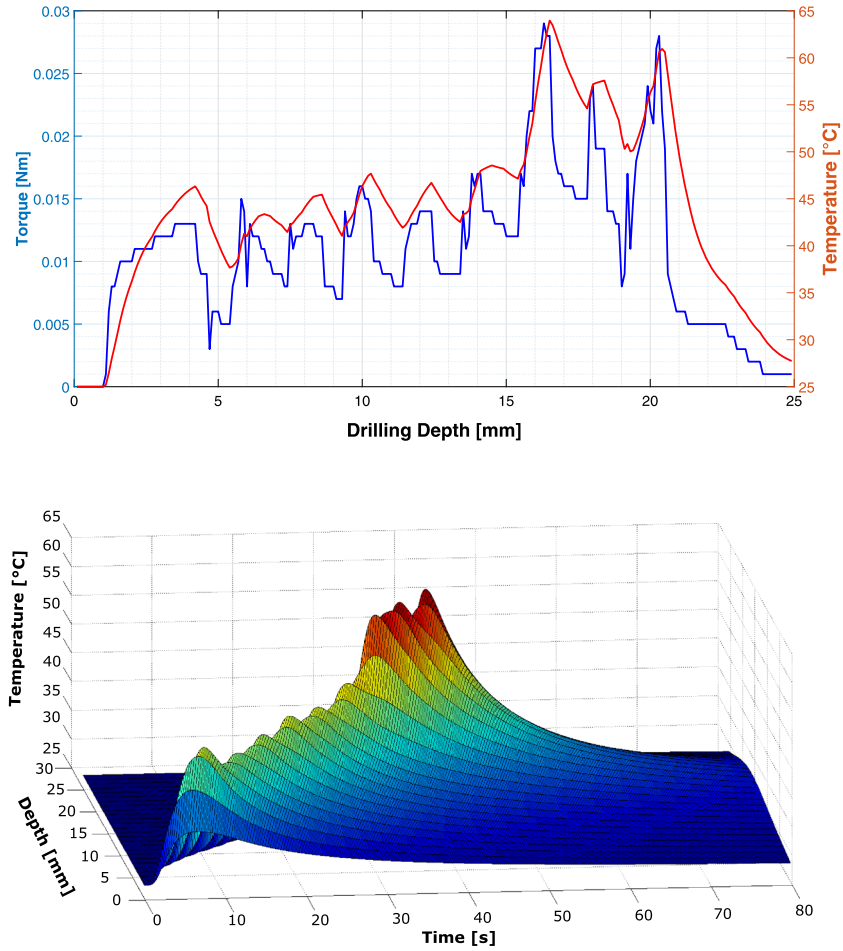


**FIGURE 4.** ***Top*** **example of measured torque and resulting maximal temperature elevation over drilling depth.** ***Bottom*** **model prediction of temperature elevation over time and drilling depth evaluated in $z_i = 1$ mm steps in the plane of thermal camera measurements. The rim of the temperature is the maximal temperature over time of the moving heat source (see 2-D plot on the** ***top*****).**

fore not be seen as absolute values but with respect to the distance of the drill bit.

## DISCUSSION

The aim of this work was to present and evaluate a model which uses the torque of a drilling process to predict the temperature elevation within the bone. This is especially important when drilling close to vulnerable structures like nerves which is, for example, necessary in minimally invasive robotic cochlear implantation. To mimic the bone anatomy for this application while allowing thermal camera temperature measurements, differently spaced lateral holes were drilled into bovine cortical bone. The average volume fractions represent approximate values commonly seen in human temporal bones, as determined from an initial analysis of bone density based on CT data. Note that no actual human temporal bones were used because of the difficulties to measure a temperature field with the porous samples. The advantages of the used thermal camera, in contrast to thermocouples, is the continuous 2-D-field measurement and the lack of contact and placement problems. However, the surface for the thermal imaging needs to be smooth, flat and dry. Thus precluding the use of temporal bone samples.

A previously proposed model[7] has been augmented to allow for measurements based on intra-operatively collected data and to account for different drill bit diameters. The model requires the calibration of only two constants for which 5 of 40 experiments were used. The calibration $(M(t)/M_0)^{(b-1)}$ describe the fraction of the work that is converted into heat and transferred to the work piece (bone). This fraction has a non-linear dependency on the amount of torque. This could be due to the changing temperature gradient for higher accoutered torques/temperatures. In general, it was found that the torque is a better indicator than the

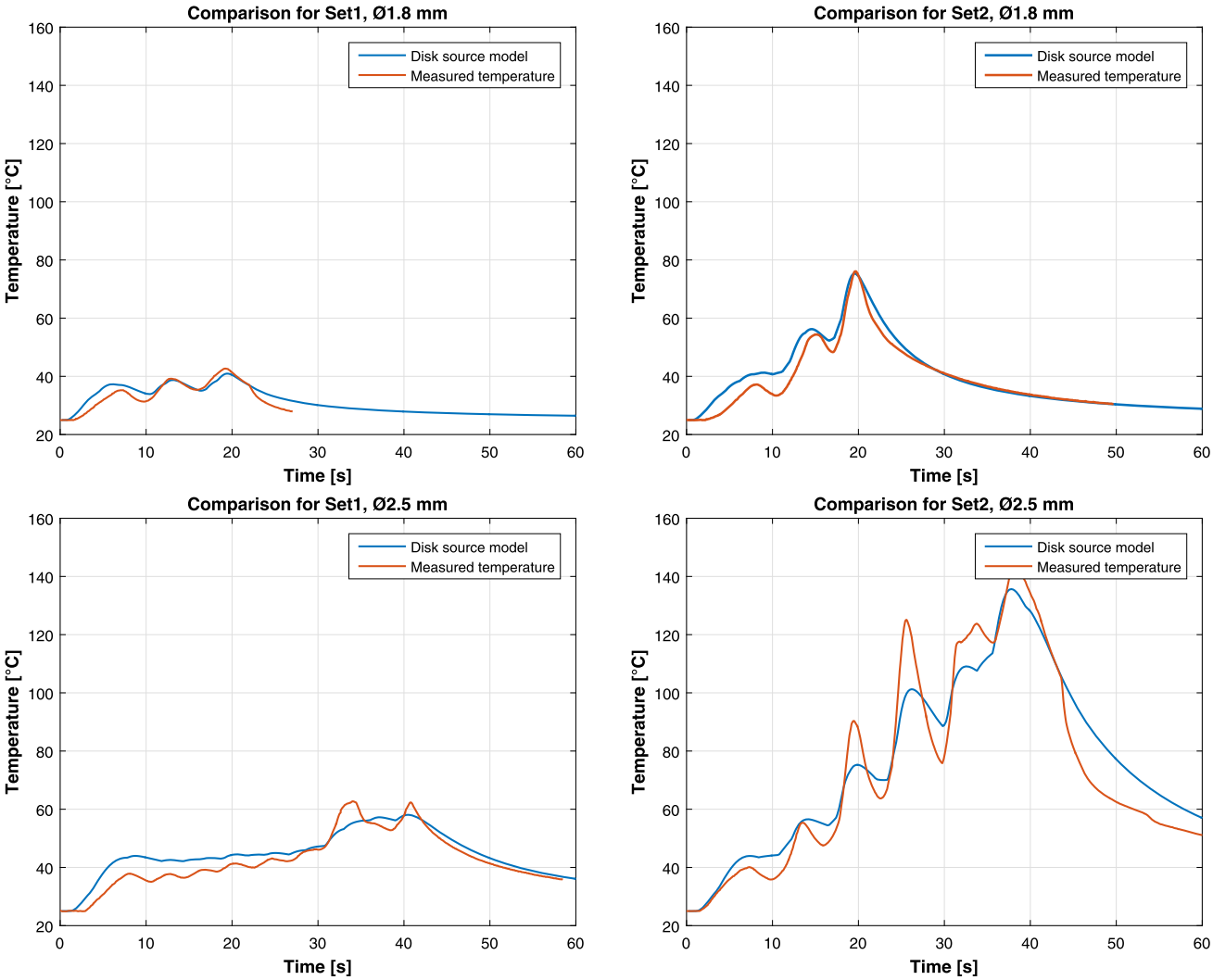


**FIGURE 5. Comparison of four examples of temperature elevation of model and measurements for both drill bits for sets 1 and 2. Drilling time and depth is double for the ∅2.5 mm compared to the ∅1.8 mm drill bit. Drill bit flutes tend to clog at high densities and drilling depths which leads to excessive temperature rise.**

thrust force of the work needed to cut and remove the material and therefore used to calculate the heat function. Nonetheless, the question remains if thrust force or torque is a better indicator for bone volume fraction as used in the previous work.[7] However, adding the thrust force to Eq. (1) does not significantly increase the temperature prediction.

The advantage of this model is however its fast computational time (within the fraction of a second for a single point) which allows real time temperature prediction and therefore a dynamic monitoring of the drilling process. Also, to our knowledge, no other model has been validated in such detail with different bone anatomies and for such deep drilling depths. A further decrease in computation time can be achieved if the model is modified to a single point source model which is possible if only drill bits with one diameter are used. This simplification does not significantly decrease the accuracy of the model. Additionally, with similar accuracy only one constant needs to be calibrated if only the torque signal is used.

The model could further be used for calculating and predicting tissue damage (cumulative equivalent minutes at 43 °C degree[22] CEM43) at a certain point (e.g., nerve position). Literature values for thermal nerve necrosis are scarce and only existed for long term damage.[11,28] However, bone necrosis starts at 47 °C for 1 min time exposure[6] or around 70 °C for instantaneous tissue damage.[25] This relates to around 55 °C maximal allowed peak temperature elevation of a temperature curve over time for a moving heat source (e.g., drill bit; from 37 °C body temperature $\Delta T = 18\,°C$).[7] Temperature predictions of the model are also more accurate when $\Delta T < 25\,°C$ (see Fig. 6)

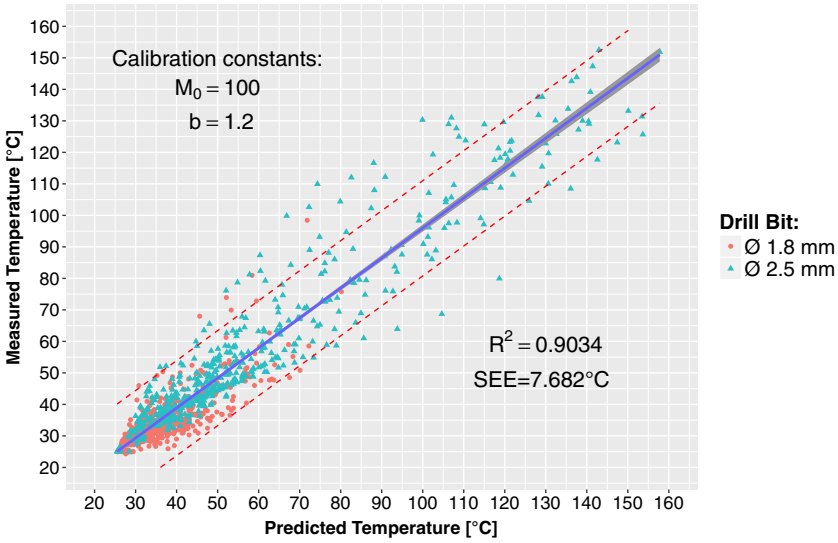


**FIGURE 6. Regression for predicted and measured temperatures using the torque to calculate the energy function. 95% Prediction and confidence intervals are shown.**

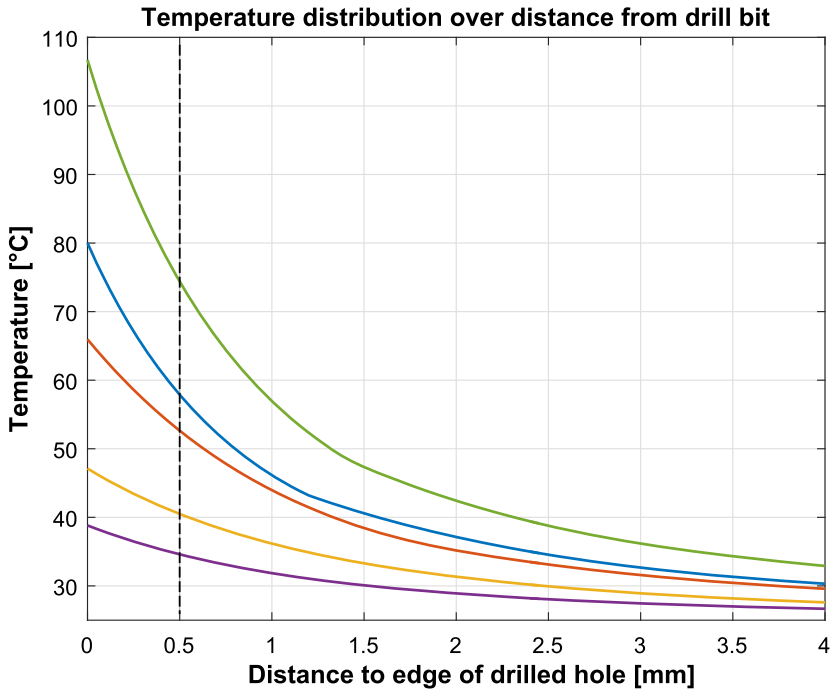


**FIGURE 7. Five random examples of temperature drop for different maximal temperatures at the drill bit as a function of distance to the drilled hole. There is a large temperature drop within only a few millimeters due to the low thermal conductivity of bone. Within this study, temperatures were evaluated at a distance of 0.5 mm the edge of the drilled hole.**

which is therefore sufficient to accurately determine the CEMs. Individual thresholds have to be defined depending on the tissue and the model can also be calibrated for a slight over-prediction to incorporate a safety threshold.

The disadvantage of the proposed model is that the calibration constants are only valid for constant process parameters and drill bit design. A re-calibration is needed if constant feed rate (or robotic movement), rotational speed, irrigation rate or drill bit design is changed. The model has also not been validated with variable (manual) feed rate and is therefore at the moment more useful for robotic surgeries.

Due to the simplicity of the model, there is a further limitation as illustrated in Fig. 8. The predicted and measured temperature elevation of three single points

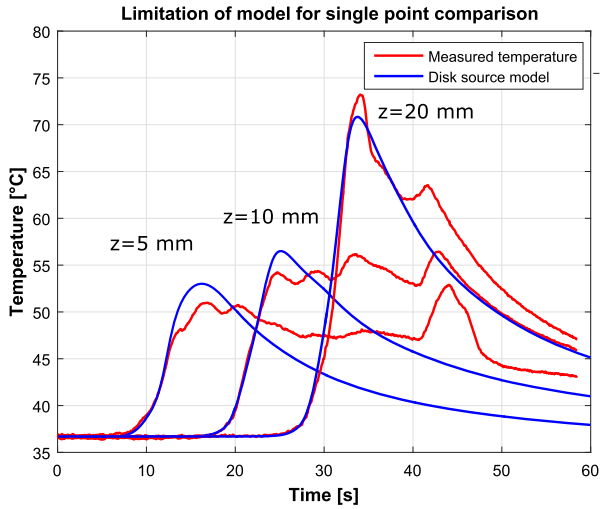


**FIGURE 8. Example of comparison of model and measurement data at three single points (5, 10 and 15 mm) over time (and shifted to body temperature). While temperature raise and maximum temperature elevation have been validated successfully, the temperature at a later time at a single point can be inaccurate. This is due to the simplicity of the model and the lack of modeling drill bit shaft conduction and evacuation of bone chip.**

at different depths (at 5, 10 and 15 mm; temperatures shifted to 37 °C) are compared. While the temperature rise and overall maximum temperature elevation can be predicted quite accurately, the temperature at a single point at a later time is in some cases predicted inaccurately. The reason for this underprediction is that the drill bit shaft conduction and evacuated chips are not modeled and can therefore not contribute to the heat of points above the drill bit tip at a later time. This could be achieved with the downside of increased computation time if this model is combined with, for example, a more detailed approach to model the drill bit as suggested by Lee *et al.*[15] Also, in the future, a $\mu$FE models of the detailed bone anatomy could be used to increase to localized prediction of temperature elevation. An inclusion of the tip shape (cone instead of disk) was tested but found to have no significant impact. The scaling of the torque with the radius (lever arm) could also be topic of further investigations. In general, this limitation is however only problematic if the tissue damage threshold is reached by an accumulation of low temperatures over a long period of time (which is most likely to happen at a shallow drilling depth).

## CONCLUSION

In this study, an analytical computational model is introduced which uses the torque signal of the drilling process in bone to predict the temperature elevation in the surrounding bone tissue. An extensive experimental study was carried out in order to calibrate and evaluate the model. It was found that the heat function and therefore temperature elevation can be predicted using only the torque and not the thrust force signal. The model was successfully validated by comparing predicted and measured maximal temperature elevations of the whole drilling depth ($R^2 = 0.9034$, $SEE = 7.682\,°C$). The advantage of this simple model is that its fast to calculate while using the real time measurements of the torque signal of a drilling process. It is however not yet possible to model the heat from the bone chips and the drill bit shaft. In the future, it could be used to monitor and control the drilling process in real-time of more delicate surgical interventions like minimally invasive robotic cochlear implantation.

## ACKNOWLEDGMENTS

The authors we would like to acknowledge Nano Tera and the Swiss National Science Foundation for funding the Research (16-954) within the Hear Restore Project (RTD 2013). Additionally, the authors would also like to thank Dr. JuEun Lee for her valuable comments during her stay in our research group.

## DISCLOSURES

We declare no conflict of interest and no ethical approval was required.

## REFERENCES

[1]Augustin, G., T. Zigman, S. Davila, T. Udilljak, T. Staroveski, D. Brezak, and S. Babic. Cortical bone drilling and thermal osteonecrosis. *Clin. Biomech. (Bristol, Avon)* 27:313–325, 2012.

[2]Bell, B., C. Stieger, N. Gerber, M. Caversaccio, and S. Weber. A self-developed and constructer robot for minimally invasive cochlear implantation. *Acta otolaryngol.* 132:355–360, 2012.

[3]Bertollo, N., and W. R. Walsh. Drilling of bone: practicality, limitations and complications associated with surgical drill-bits. In: Biomechanics in Applications, edited by V. Klika. InTech, 2011. doi:10.5772/20931.

[4]Chen, H. L., and A. A. Gundjian. Specific heat of bone. *Med. Biol. Eng.* 14:548–550, 1976.

[5]Davidson, S. R., and D. F. James. Measurement of thermal conductivity of bovine cortical bone. *Med. Eng. Phys.* 22:741–747, 2000.

[6]Eriksson, R., and T. Albrektsson. The effect of heat on bone regeneration: an experimental study in the rabbit using the bone growth chamber. *J. Oral Maxillofac. Surg.* 42:705–711, 1984.

[7]Feldmann, A., J. Anso, B. Bell, T. Williamson, K. Gavaghan, N. Gerber, H. Rohrbach, and P. Zysset. Temperature prediction model for bone drilling based on density distribution and in vivo experiments for minimally invasive robotic cochlear implantation. *Ann. Biomed. Eng*. 44:1576–1586, 2015.
[8]Feldmann, A., J. Wandel, and P. Zysset. Reducing temperature elevation of robotic bone drilling. *Med. Eng. Phys*. 38: 1495–1504, 2016.
[9]Feldmann, A., and P. Zysset. Experimental determination of the emissivity of bone. *Med. Eng. Phys*. 38:1136–1138, 2016.
[10]Gulya, A. J., and H. Schuknecht. Anatomy of the Temporal Bone with Surgical Implications, 3rd edition. Washington, DC: Informa Healthcare, 2007.
[11]Havemann, J., J. van der Zee, and J. Wondergems. Effects of hyperthermia on the peripheral nervous system: a review. *Int. J. Hyperth*. 20:371–391, 2004.
[12]Klocke, F., and W. König. Fertigungsverfahren 1 - Drehen, Fräsen, Bohren, 8th edition. Aachen: Springer, RWTH Aachen, 2008.
[13]Labadie, R. F., R. Balachandran, J. H. Noble, G. S. Blachon, J. E. Mitchell, F. A. Reda, B. M. Dawant, and J. M. Fitzpatrick. Minimally invasive image-guided cochlear implantation surgery: first report of clinical implementation. *Laryngoscope* 124:1–8, 2014.
[14]Lee, J., B. A. Gozen, and O. B. Ozdoganlar. Modeling and experimentation of bone drilling forces. *J. Biomech*. 45:1076–1083, 2011.
[15]Lee, J., Y. Rabin, and O. B. Ozdoganlar. A new thermal model for bone drilling with applications to orthopaedic surgery. *Med. Eng. Phys*. 33:1234–1244, 2011.
[16]Lughmani, W., K. Bouazza-Marouf, and I. Ashcroft. Drilling in cortical bone: a finite element model and experimental investigations. *J. Mech. Behav. Biomed. Mater*. 42:32–42, 2015.
[17]Maani, N., K. Farhang, and M. Hodaei. A model for the prediction of thermal response of bone in surgical drilling. *J. Therm. Sci. Eng. Appl*. 6:1–17, 2014.
[18]Marco, M., M. Rodriguez-Millan, C. Santiuste, E. Giner, and M. H. Miguelez. A review on recent advances in numerical modelling of bone cutting. *J. Mech. Behav. Biomed. Mater*. 44:179–201, 2015.
[19]Nagao, T., and Y. Hatamura. Investigation into drilling laminated printed circuit board using a torque–thrust–temperature sensor. *Ann. CIRP* 37:79–82, 1988.
[20]Paek, U., and F. Gagliano. Thermal analysis of laser drilling process. *IEEE J. Quantum Electron*. 8:112–119, 1972.
[21]Pandey, R. K., and S. Panda. Drilling of bone: a comprehensive review. *J. Clin. Orthop. Trauma* 4:15–30, 2013.
[22]Sapareto, S. A., and W. C. Dewey. Thermal dose determination in cancer therapy. *Int. J. Radiat. Oncol. Biol. Phys*. 10:787–800, 1984.
[23]Sezek, S., B. Aksakal, and F. Karaca. Influence of drill parameters on bone temperature and necrosis: a FEM modelling and in vitro experiments. *Comput. Mater. Sci*. 60:13–18, 2012.
[24]Sui, J., N. Sugita, K. Ishii, K. Harada, and M. Mitsuishi. Mechanistic modeling of bone-drilling process with experimental validation. *J. Mater. Process. Technol*. 214:1018–1026, 2013.
[25]Tai, B., A. Palmisano, B. Belmont, T. Irwin, J. Holmes, and A. Shih; Numerical evaluation of sequential bone drilling strategies based on thermal damage; Medical Engineering and Physics; 37:885–861; 2015.
[26]Trisi, P., and G. Perfetti. Insufficient irrigation induces peri-implant bone resorption: an in vivo histologic analysis in sheep. *Clin. Oral Implants Res*. 25:696–701, 2014.
[27]Tu, Y.-K., W.-H. Lu, L.-W. Chen, J.-S. Ciou, and Y.-C. Chen. The effects of drilling parameters on bone temperatures: a finite element simulation. In: 2011 5th International Conference on Bioinformatics and Biomedical Engineering, 2011, pp. 1–4.
[28]de Vrind, H. H., J. Wondergem, and H. de Vrind. Hyperthermia-induced damage to rat sciatic nerve assessed in vivo with functional methods and with electrophysiology. *J. Neurosci. Methods* 45:165–174, 1992.
[29]Williamson, T. M., B. J. Bell, N. Gerber, L. Salas, P. Zysset, M. Caversaccio, and S. Weber. Estimation of tool pose based on force–density correlation during robotic drilling. *IEEE Trans. Biomed. Eng*. 60:969–976, 2013.